Science of Sintering, **39** (2007) 153-160

doi:10.2298/SOS0702153I

UDK 662.785:661.847.2:546.812:77.026.34

Investigation of Zinc Stannate Synthesis Using Photoacoustic Spectroscopy

T. Ivetić[1*)], M. V. Nikolić[2], P. M. Nikolić[1], V. Blagojević[3], S. Đurić[1], T. Srećković[2], M. M. Ristić[1]

[1]Institute of Technical Sciences of the Serbian Academy of Sciences and Arts, Knez Mihailova 35/IV, 11000 Belgrade, Serbia

[2]Center for Multidisciplinary Studies of the University of Belgrade, Kneza Višeslava 1, 11000 Belgrade, Serbia

[3]Faculty of Electrical Engineering, University of Belgrade, Bulevar Kralja Aleksandra 73, 11000 Belgrade, Serbia

Abstract:

Mixtures of ZnO and SnO_2 powders, with molar ratio of 2:1, were mechanically activated for 40, 80 and 160 minutes in a planetary ball mill. The resulting powders were compacted into pellets and non-isothermally sintered up to 1200˚C with a heating rate of 5˚C/min. X-ray diffraction analysis of obtained powders and sintered samples was performed in order to investigate changes of the phase composition. The microstructure of sintered samples was examined by scanning electron microscopy. The photoacoustic phase and amplitude spectra of sintered samples were measured as a function of the laser beam modulating frequency using a transmission detection configuration. Fitting of experimental data enabled determination of photoacoustic properties including thermal diffusivity. Based on the results obtained a correlation between thermal diffusivity and experimental conditions as well the samples microstructure characteristics was discussed.

Keywords: *Zinc Stannate, Mechanical activation, Sintering, Photoacoustic spectroscopy*

Introduction

Ceramic materials with large open porosity, such as zinc stannate (Zn_2SnO_4) obtained in this paper from the reaction sintering powder-processing route, are convenient for use as humidity sensors. Atmospheric water can be absorbed on the grain surface inside pores or can be condensed in small channels and pores. Desirable characteristics of humidity sensors include: high sensitivity, reversibility, fast response, broad range of moisture selectivity, chemical and thermal stability. These sensor characteristics depend upon parameters of synthesis during the reaction sintering process. Knowing the thermal properties of this kind of material is very important, especially when they are used as electrical components because of the need for an adequate cooling process. In this paper, we present the results of a photoacoustic investigation of thermal and transport properties of bulk zinc stannate synthesized by the reaction sintering process. Photoacoustic (PA) spectroscopy has been used lately, besides for the characterization of electronic, optical and defects structures, for

*) Corresponding author: tamara@itn.sanu.ac.yu

defining the electronic states and structural disorders of ceramic materials [1-4]. In a typical photoacoustic experiment the sample is placed in a closed photoacoustic cell exposed to radiation with a modulated laser beam [5]. The dependence of the obtained photoacoustic signal on the rate of diffunded heat through the sample enables thermal characterization of the sample, i.e. determination of different properties of the analyzed material including thermal diffusivity [3]. The PA signal is a consequence of heat processes in the observed sample. It depends on periodic temperature variation on the rear sample surface, $\Phi\ (-l,\omega)$ that is in contact with the electret microphone (Fig. 1.).

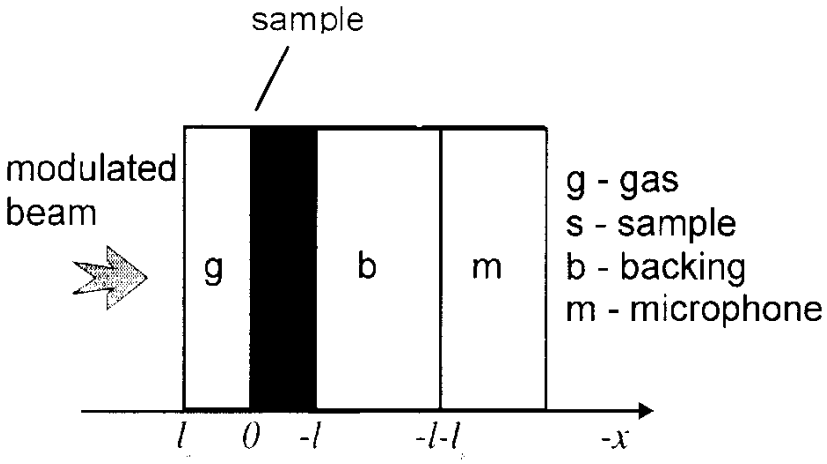

Fig. 1 The gas-sample-backing-microphone detection configuration.

The following relation can express the PA signal:

$$S(\omega)=\frac{\gamma\cdot P_0}{T_0\cdot k(\omega)\cdot l_b}\Phi(-l,\omega) \qquad (1)$$

Where l is the sample thickness; ω is the frequency modulation of the excitation light beam; γ is the adiabatic constant and P_0 and T_0 are ambient pressure and temperature, respectively; $k_b(\omega)=(1+j)/\mu_b(\omega)$, where $\mu_b(\omega)$ is the thermal diffusion length of the backing (gas); l_b is the distance between the sample and microphone membrane and $\Phi(l,\omega)$ is the temperature variation of the sample surface that is in contact with microphone.

Experimental

Commercially available zinc oxide and tin oxide powders (Aldrich), with a molar ratio $ZnO:SnO_2$ = 2:1, were mechanically activated in a planetary ball mill (Fritsch Pulverisette 5) in the continuous grinding process regime, in air for 40, 80 and 160 min. Zirconium oxide grinding balls (10 mm in diameter, approx.) and vessels (500 cm^3) were used. The powder to balls ratio was 40:1 and the total weight of the powder mixtures was 10 g. Appropriate samples were denoted according to the applied time of activation as ZSO-40, ZSO-80 and ZSO-160. These samples were uniaxially pressed with different pressures (ZSO-40 – 150 MPa, ZSO-80, ZSO-160 – 200 MPa) in accordance with the analysis of the influence of mechanical activation on consolidation of the $ZnO\text{-}SnO_2$ system given in detail in [6] in order to obtain the same average green density of 3.769 g/cm^3. Relative shrinkage of samples obtained by uniaxial pressing of activated powders was measured by a sensitive dilatometer (Bähr Gerätebau GmbH Typ 702s) in the course of non-isothermal heating in air

up to 1200˚C with a constant heating rate of 5˚C/min. The densities of sintered samples were determined and the values obtained are given in Tab. I. Characterization of the obtained samples of powder mixtures after grinding and after sintering was carried out using an X-ray diffractometer (Norelco-Philips PW-1050) with CuK_α radiation and a step scan mode of 0.02º/0.4s. The microstructure of sintered samples was characterized using scanning electron microscopy (SEM – JSM 5300 JEOL).

Tab. I Measured density and calculated thermal diffusivity of ZSO samples sintered at 1200˚C

Milling time	Density (g/cm^3)	D_T (m^2s^{-1})	D (m^2s^{-1})	α (m^{-1})
40	4.14	$0.21 \cdot 10^{-7}$	$0.25 \cdot 10^{-5}$	9860
80	4.12	$1.80 \cdot 10^{-7}$	$0.10 \cdot 10^{-5}$	12400
160	3.86	$10.06 \cdot 10^{-7}$	$0.14 \cdot 10^{-4}$	11000

The PA signals were measured using an experimental set-up, with an infrared laser (25 mW) as the optical source. The laser beam was modulated with a mechanical chopper. Changes in phases and amplitudes of the photoacoustic signal of obtained sintered samples were followed.

Results and discussion

X-ray diffraction patterns of ZSO powder mixtures are shown on Fig. 2. Mechanical activation of ZnO and SnO_2 powders, results in the start of formation of zinc stannate after 40 minutes of milling (this time was denoted in [7] as the shortest milling time needed for the beginning of zinc-stannate formation), but as the XRD patterns obtained show residual oxides are still present. Longer milling times result in lower amounts of residual oxides present. Formation of Zn_2SnO_4 is not yet finished after 160 minutes of ball milling, as SnO_2 is still present.

Fig. 3 shows XRD patterns of powder mixtures after uniaxial pressing and non-isothermal sintering up to 1200˚C with a constant heating rate of 5˚C/min. The peaks from the XRD spectra of samples sintered up to 1200˚C are much sharper and better defined from the non-sintered ones indicating creation of monophased spinel zinc stannate. Only a few peaks derived from residual oxides are present in the ZSO-40 sample and only one ZnO peak developed in the sample mechanically activated for 80 minutes while the ZSO-160 sample shows only the zinc-stannate phase.

SEM microphotographs of fractured surfaces of ZSO powder samples non-isothermally sintered in a dilatometer up to 1200˚C with a heating rate of 5˚C/min are presented in Fig. 4-6. SEM microphotographs show that grinding leads to the formation of a structure with a reduced grain size that accelerates spinel formation (which is with agreement with XRD analysis), but agglomerates are also present, probably preserved from the agglomeration of powders. Grain growth of spinel inhibits densification and causes the formation of a porous microstructure.

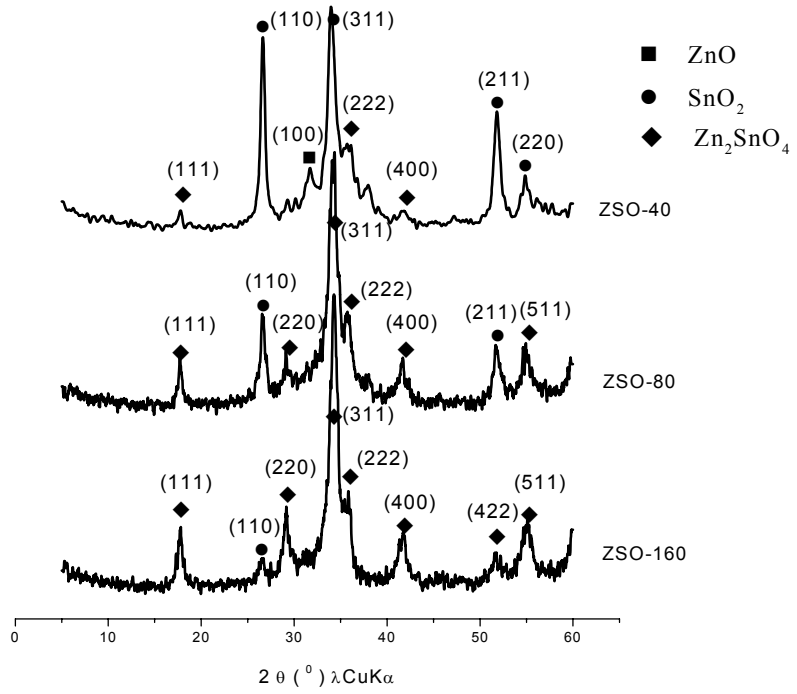

Fig. 2 XRD patterns of ZSO powder mixtures as a function of the activation time.

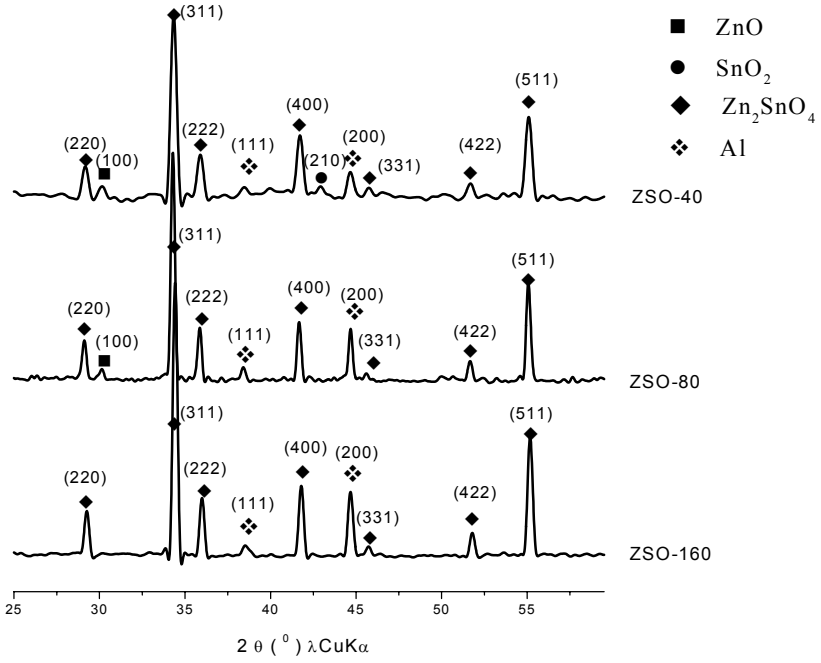

Fig. 3 XRD patterns of ZSO samples non-isothermally sintered up to 1200˚C with a heating rate of 5˚C/min.

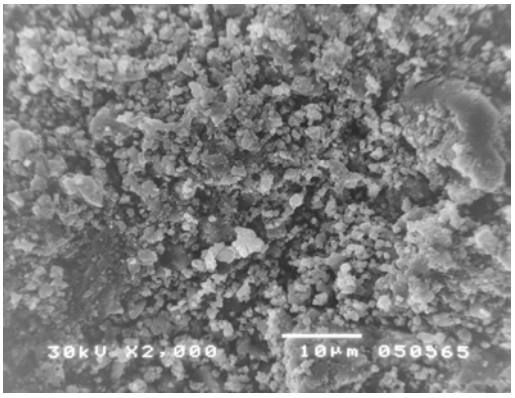

Fig. 4 SEM fractured surface of the ZSO-40 sample sintered at 1200˚C.

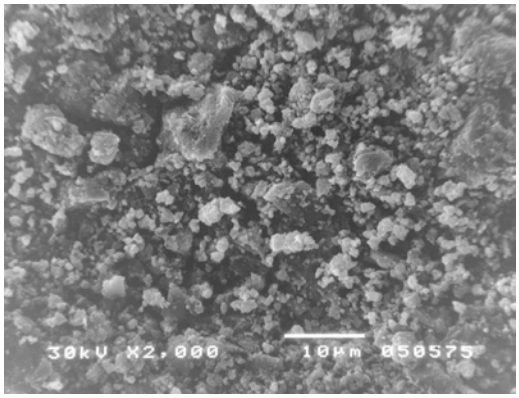

Fig. 5 SEM fractured surface of the ZSO-80 sample sintered at 1200˚C

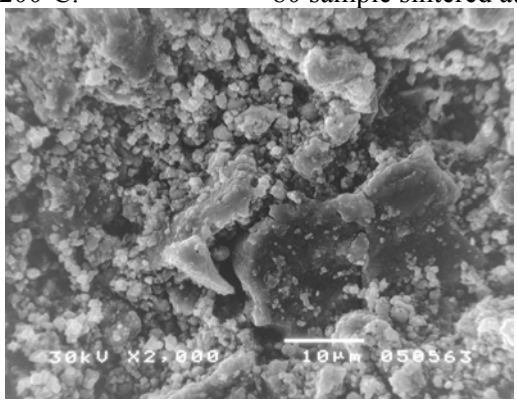

Fig. 6 SEM fractured surface of the ZSO-160 sample sintered at 1200˚C.

Fig. 7 shows the relative shrinkage of samples as a function of temperature during heating for the different activated samples (ZSO-40, ZSO-80 and ZSO-160) obtained by the dilatometer. Dilatometric curves confirm the XRD analysis results that the formed spinel phase dominates in the system so there is no trace of other processes but sintering. It is interesting to note that shrinkage is the highest for the sample mechanically activated for the shortest time and the lowest for the sample activated for the longest time. This is in accordance with the density values obtained (Tab. I), where densities increase is noted for all samples during sintering, but it is the highest for the ZSO-40 sample. This can be attributed to different particle packing during uniaxial pressing. Also, the formation of spinel with increasing activation time could inhibit densification (sintering process).

A theoretical analysis of the experimental PA results was performed following the Rosencwaig–Gersho thermal piston model [8-9] where a complex system in the gas–sample–backing–microphone configuration given in Fig. 1 is considered.

Experimental photoacoustic phase and amplitude diagrams were fitted with theoretical calculated photoacoustic signals for zinc stannate. Fig. 8 shows the measured and calculated phase and amplitude of the photoacoustic spectra for the zinc stannate sample activated for 160 min. A fitting procedure described in detail in [4] was used for determining thermal parameters of zinc stannate, including thermal diffusivity D_T (m^2s^{-1}), then the diffusion coefficient of the minority free carriers D (m^2s^{-1}) and optical absorption coefficient α (m^{-1}). The obtained values are given in Tab. I.

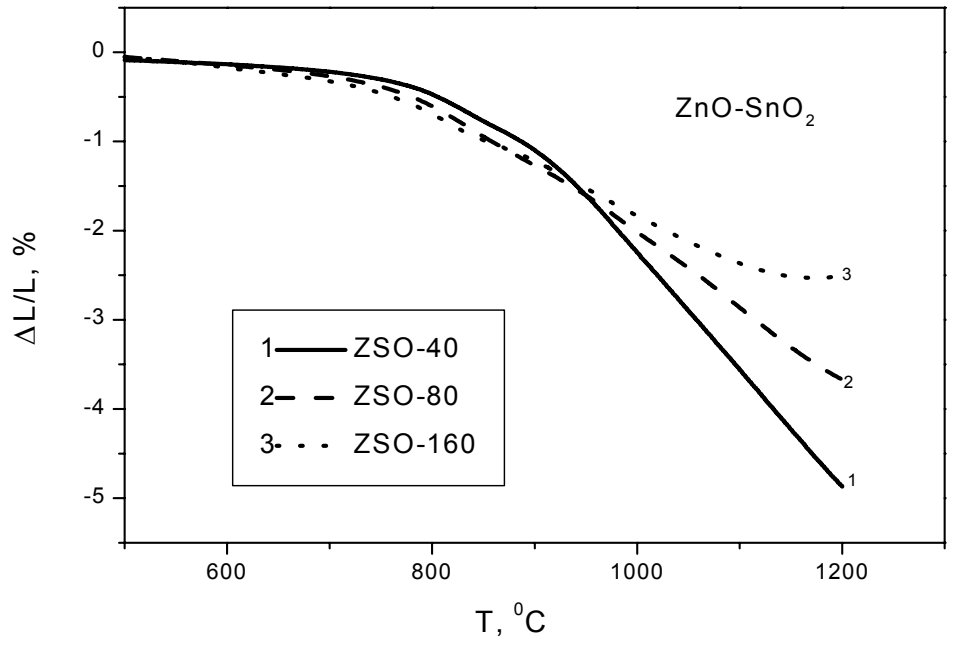

Fig.7 Relative shrinkage of ZSO samples as a function of the heating temperature and the activation time during non-isothermal sintering up to 1200˚C with a heating rate of 5˚C/min.

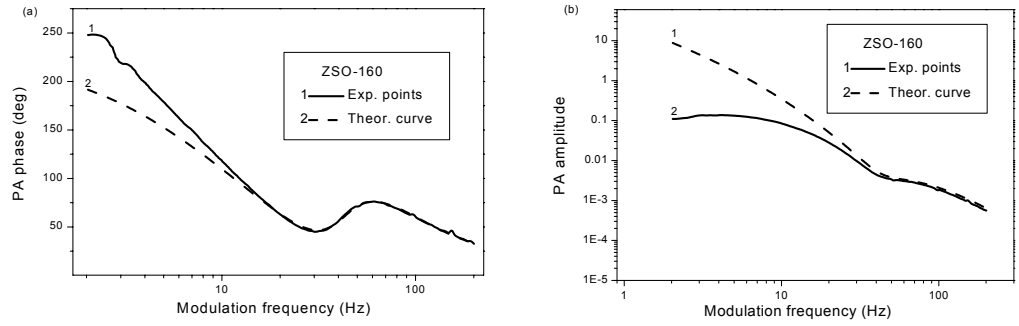

Fig. 8 (a) Phase photoacoustic spectra for ZSO-160 sample, (b) Amplitude photoacoustic spectra for ZSO-160 sample.

With the increase of activation time and the amount of the zinc stannate phase present the thermal diffusivity value increases. The value of thermal diffusivity obtained for ZSO-160 (pure zinc stannate phase) is almost identical to the thermal diffusivity value we calculated for thin film zinc stannate [10]. To our best knowledge no other thermal diffusivity values for Zn_2SnO_4, synthesized in this way, are available in the literature.

Conclusion

In this paper synthesis of zinc-stannate was analyzed using photoacoustic spectroscopy. Mixtures of ZnO and SnO_2 were mechanically activated for 40, 80 and 160 minutes in a planetary ball mill and then non-isothermally sintered up to 1200°C. X-ray diffraction analyses confirmed the beginning of zinc-stannate formation in the milled powders and a pure zinc-stannate phase in the sample mechanically activated for 160 min. and then sintered. The photoacoustic phase and amplitude diagrams of sintered zinc stannate samples were measured in relation to the frequency of the chopped laser beam. It was shown that thermal diffusivity of this material increased with the activation time in accordance with the formation of single phase Zn_2SnO_4.

Acknowledgement

This research was performed as part of project 142011G financed by the Ministry for Science of the Republic of Serbia and project F-198 of Serbian Academy of Sciences and Arts.

References

1. T. Toyoda, S. Shimamoto, Mater. Sci. Eng. B, 54 (1998) 29.
2. J. Soldner, K. Stephan, Chem. Eng. Process., 38 (1999) 585.
3. N. A. George, T. Paul, P. Radhakrishnan, V. P. N. Nampoori, C. P. G. Vallabhan, M. T. Sebastian, J. Mater. Sci. Lett., 19 (2000) 499.
4. P. M. Nikolić, D. Vasiljević, M. Miletić, Glas CCCLXXX of the Serbian Academy of Sciences and Arts, Department of Technical Sciences, 32 (1996) 27.
5. D. M. Todorović, P. M. Nikolić, Opt. Eng., 36 (1997) 432.
6. T. B. Ivetić, K. M. Vojisavljević, T. Srećković, in: "Fundamental Problems of Physics and Technology of Materials", Eds. M. M. Ristić and A. M. Maričić, Čačak, 2005, p. 115-121.
7. N. Nikolić, Z. Marinković, T. Srećković, J. Mat. Sci., 39 (2004) 5239.
8. P. M. Nikolić, M. V. Nikolić, D. Luković, S. Savić, M. M. Ristić, Z. Metallkd., 95 (2004) 147.
9. A. Rosencwaig, A. Gersho, J. Appl. Phys., 47 (1976) 11.
10. T. Ivetić, M. V. Nikolić, D. L. Young, D. Vasiljević-Radović, D. Urošević, Mater. Sci. Forum, 518 (2006) 465.

Садржај:. *Смеше прахова цинк-оксида и калај-оксида помешане су у молском односу 2:1 и механички активиране 40, 80 и 160 минута у планетарном млину са куглама. Добијени прахови пресовани су и неизотермски синтеровани до 1200ºC брзином загревања од 5ºC/мин. Квалитативни састав полазних смеша прахова и синтерованих узорака одређен је методом рендгенске дифракције. Еволуција микроструктуре синтерованих узорака испитана је сканирајућом електронском микроскопијом. Фотоакустични фазни и амплитудски спектри синтерованих узорака снимани су у функцији чоповане фреквенције употребљеног ласерског зрачења у топлотно-трансмисионој конфигурацији. Теоријска анализа експерименталних резултата омогућила је израчунавање фотоакустичних својстава материјала укључујући и*

топлотну дифузивност. На основу добијених резултата испитана је повезаност експерименталних услова припреме узорака и њихове микроструктуре.
***Кључне речи**: Цинк-станат, механичка активација, синтеровање, фотоакустична спектроскопија.*